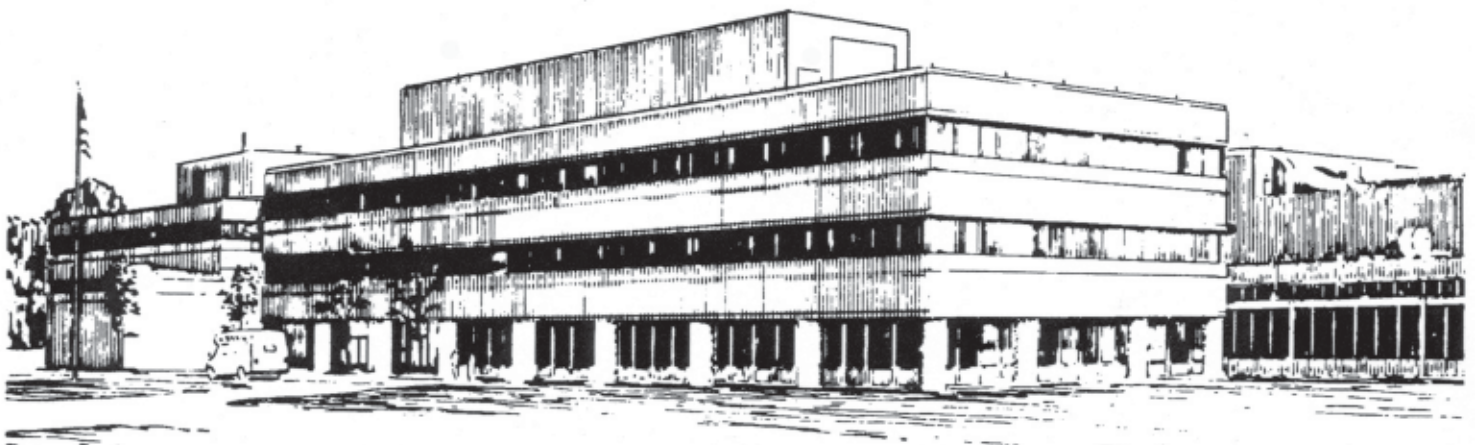# Initial Neutral Particle Analyzer Measurements of Ion Temperature in NSTX

by

S.S. Medley, R.E. Bell, M.P. Petrov,
A.L. Roquemore, and E.V. Suvorkin

July 2002

**PPPL
PRINCETON PLASMA
PHYSICS LABORATORY**

PPPL Reports Disclaimer

This report was prepared as an account of work sponsored by an agency of the United States Government. Neither the United States Government nor any agency thereof, nor any of their employees, makes any warranty, express or implied, or assumes any legal liability or responsibility for the accuracy, completeness, or usefulness of any information, apparatus, product, or process disclosed, or represents that its use would not infringe privately owned rights. Reference herein to any specific commercial product, process, or service by trade name, trademark, manufacturer, or otherwise, does not necessarily constitute or imply its endorsement, recommendation, or favoring by the United States Government or any agency thereof. The views and opinions of authors expressed herein do not necessarily state or reflect those of the United States Government or any agency thereof.

Availability

This report is posted on the U.S. Department of Energy's Princeton Plasma Physics Laboratory Publications and Reports web site in Fiscal Year 2002. The home page for PPPL Reports and Publications is: http://www.pppl.gov/pub_report/

DOE and DOE Contractors can obtain copies of this report from:

U.S. Department of Energy
Office of Scientific and Technical Information
DOE Technical Information Services (DTIS)
P.O. Box 62
Oak Ridge, TN 37831

Telephone: (865) 576-8401

Fax: (865) 576-5728

Email: reports@adonis.osti.gov

This report is available to the general public from:

National Technical Information Service
U.S. Department of Commerce
5285 Port Royal Road
Springfield, VA 22161

Telephone: 1-800-553-6847 or
(703) 605-6000

Fax: (703) 321-8547

Internet: http://www.ntis.gov/ordering.htm

Initial Neutral Particle Analyzer Measurements of Ion Temperature in NSTX

S. S. Medley, R. E. Bell, M. P. Petrov[+], A. L. Roquemore and E. V. Suvorkin[+]

Princeton Plasma Physics Laboratory, Princeton, New Jersey, 08543, USA
[+] A. F. Ioffe Physical-Technical Institute, St. Petersburg 194021, Russia

Abstract

The Neutral Particle Analyzer (NPA) diagnostic on the National Spherical Torus Experiment (NSTX) utilizes a PPPL-designed E||B spectrometer which measures the energy spectra of minority H and bulk D species simultaneously with 39 energy channels per mass specie and a time resolution of 1 msec. The calibrated energy range is E = 0.5 – 150 keV and the energy resolution varies from $\Delta E/E$ = 3-7% over the surface of the microchannel plate detector. The NPA measures thermal Maxwellian ion spectra to obtain line integrated ion temperatures, T_i. For line integral electron densities below $n_e L \sim 3.5$ x 10^{19} m^{-2}, good agreement is observed between the line integrated NPA T_i and the central $T_i(0)$ measured by the spatially localized CHarge Exchange Recombination Spectroscopy (CHERS) diagnostic. However, with increasingly higher $n_e L$ the NPA T_i falls below the central $T_i(0)$ measured by CHERS because the charge exchange neutral emissivity weights the line integrated NPA measurement outboard of the plasma core. An analytic neutral analysis code, DOUBLE, has been applied to the NPA data to correct for this effect and restore agreement with $T_i(0)$ measured by CHERS. A description of the NPA diagnostic on NSTX and initial ion temperature measurements along with an illustration of application of the DOUBLE code are presented.

1.0 Introduction

The National Spherical Torus Experiment (NSTX) is a low aspect ratio ($R/a \sim 1.3$) device with auxiliary heating from Neutral Beam Injection (NBI) and High Harmonic Fast Wave (HHFW) heating. Typical NSTX parameters are R_0 = 85 cm, a = 67 cm, I_p = 0.7-1.4 MA, B_f = 0.35-0.60 T. Three co-directed deuterium neutral beam sources have injected up to $P_{NB} \sim$ 7 MW at injection energies up to $E_{NB} \sim$ 100 keV. HHFW heating at $f_{RF} \sim$30 MHz has delivered up to $P_{RF} \sim$6 MW to D and He plasmas. Important to the understanding of ion behavior in NSTX are the Neutral Particle Analyzer (NPA) and the Charge Exchange Recombination Spectroscopy (CHERS) diagnostics. The NPA diagnostic utilizes a PPPL-designed E||B spectrometer[1] which measures the energy spectra of H$^+$ and D$^+$ ion species simultaneously with a time resolution of ~1 msec set by signal-to-noise levels. The calibrated energy range is E = 0.5 – 150 keV and the energy resolution varies from $\Delta E/E$ = 7% at low E to $\Delta E/E$ = 3% at high E. The detector consists of a large area microchannel plate (MCP) which is provided with two rectangular, semi-continuous active area strips, one coinciding with each of the mass rows for detection

of H$^+$ and D$^+$ and each mass row has 39 energy channels. The NPA measures Maxwellian spectra of residual H$^+$ to obtain ion temperatures, T_i, and D$^+$ energetic ion spectra produced by injection of up to 100 keV D neutral beams into a D plasma. The CHERS system[2] measures carbon ion temperature, $T_{i,}(r)$, and toroidal flow, $V_f (r)$, during NBI at 17 radial positions spanning the outer half of the minor radius with 20 ms time resolution.
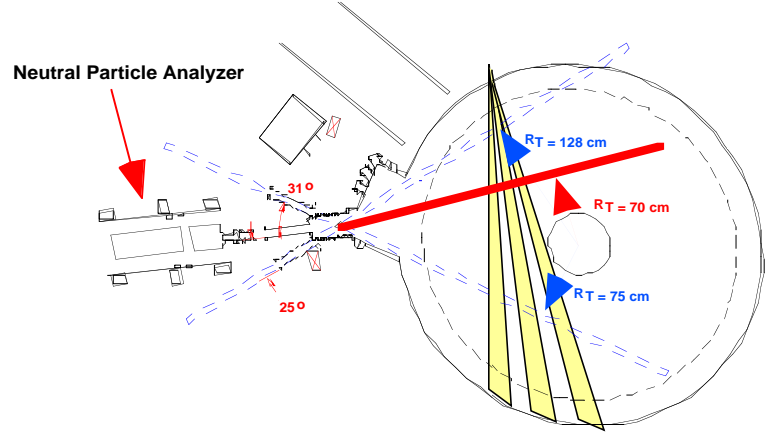

Figure 1. Layout of the Neutral Particle Analyzer on NSTX.

The three neutral beam lines on NSTX inject at R_{tan} of 70 cm (source A), 60 cm (source B) and 50 cm (source C). Initially, the NPA was installed with a fixed sightline having R_{tan} = 70 cm which views across the neutral beam lines at co-directed ions as shown by the solid chord in Figure 1. Subsequently, the NPA was upgraded to provide horizontal scanning as shown by the dashed chords as well as vertical scanning to view below the plasma midplane.

2.0 NPA Ion Temperature Measurements

Since NSTX uses deuterium for both the neutral beams and the plasma discharge, it is necessary to measure the spectra of the residual H$^+$ ions in order to obtain NPA ion temperature measurements. An example of the NPA time evolution of T_i is shown in the upper panel of Figure 2 for NSTX discharge SN106031 along with the CHERS central ion temperature, $T_i(0)$. Examples of the NPA thermal hydrogen ion spectra are presented later in this paper. The center panel shows waveforms for electron temperature and density from the Multi-Pulse Thomson Scattering (MPTS) system as well as the injected neutral beam power, plasma current and a Mirnov coil trace indicating magnetohydrodynamic (MHD) activity. The CHERS profiles during NB heating show T_i profiles that are typically hotter and broader than T_e profiles [2] as shown in the bottom panel of Figure 2 for time t = 270 msec in the discharge. The agreement of the line-integral NPA T_i measurements with the localized CHERS central ion temperature, $T_i(0)$, is no doubt abetted by the broadness of the T_i profiles.

It can be seen that the line integrated NPA and core CHERS ion temperature measurements are in good agreement up to t ~ 230 msec, after which time the data for the NPA falls below that for
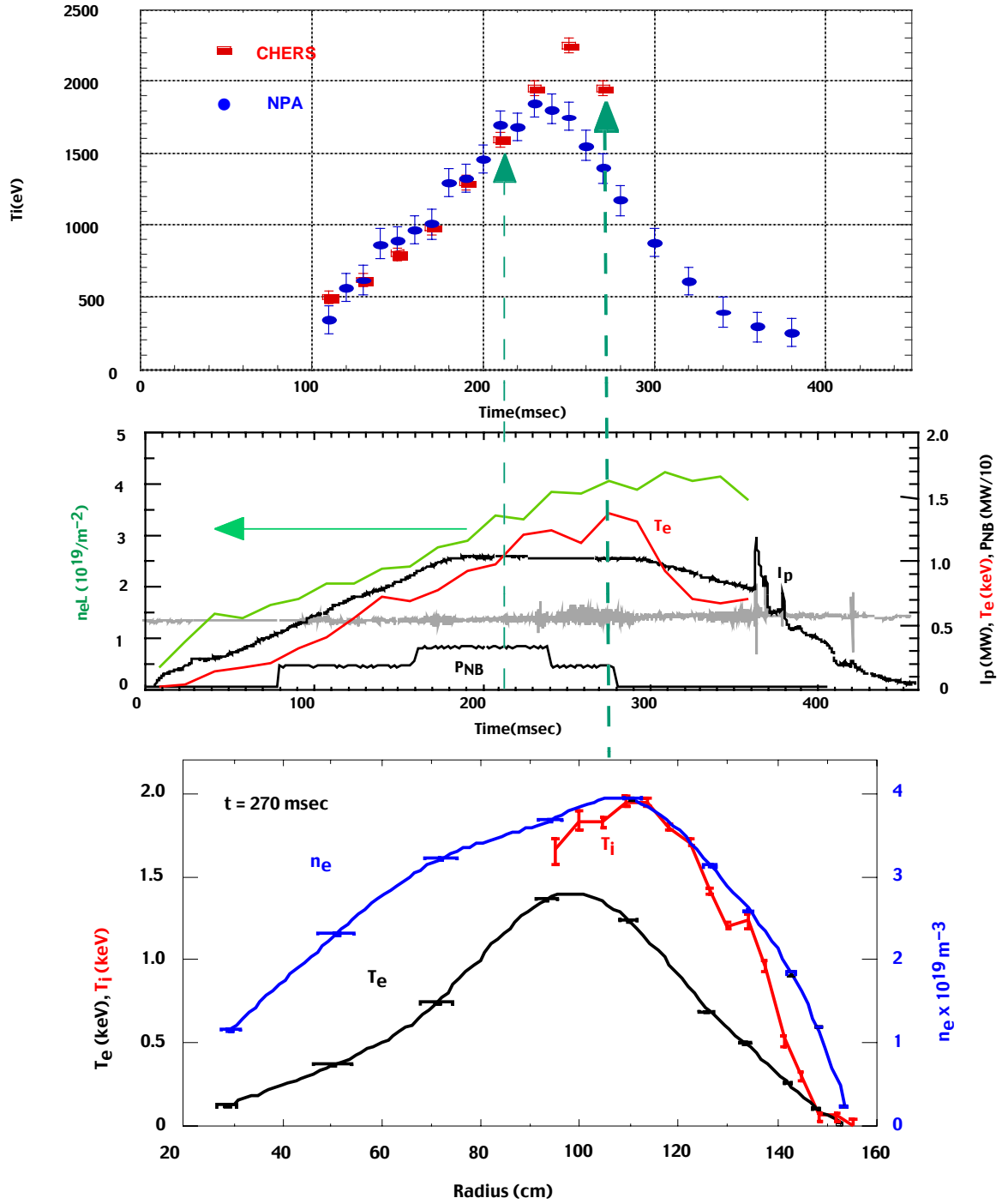
2

Figure 2. Ion temperature evolution measured by the NPA and CHERS diagnostics for discharge SN106031 (top panel), selected discharge waveforms (center panel). Multi-Pulse Thomson Scattering(MPTS) profiles of n_e and T_e and the CHERS T_i profile are shown in the bottom panel for time t = 270 msec.

3

CHERS. To examine this behavior further, a data base of NPA and CHERS measurements comprised of 12 discharges with ion temperatures measured at ~ 8 time points in each discharge was constructed. The result shown in Figure 3 reveals that the two measurements are in reasonable agreement (indicated by the dashed line) for ion temperatures up to ~ 1500 eV, above which the core CHERS value exceeds that of the line-integrated NPA. By examining the database electron density traces such as shown in the center panel of Figure 2, it was established that this roll off correlated with the line integral density exceeding n_eL ~ 3.5 x 10^{19} m^{-2}.

It is a well know shortcoming of line-integrated NPA ion temperature measurements that if the plasma opacity, $\bar{n}_e \sigma_{CX}$ a, becomes too large [3] then the observed T_i underestimates the core $T_i(0)$. If the neutral flux is sufficiently large to enable ion temperature measurements in the energy range $E/T_i(0)$ ~ 5 – 10, then T_i from the slope of the NPA thermal ion spectrum differs from $T_i(0)$ by not more than 10 – 15 % up to a plasma average density given by $\bar{n}_e \sigma_{CX}$ a ~ 10 which for NSTX would be $\bar{n}_e$ ~ 10^{20} m^{-3}. However, because the residual H^O density in NSTX is low (H^O/ D^O ~ 5%), the neutral flux is adequate to measure T_i only
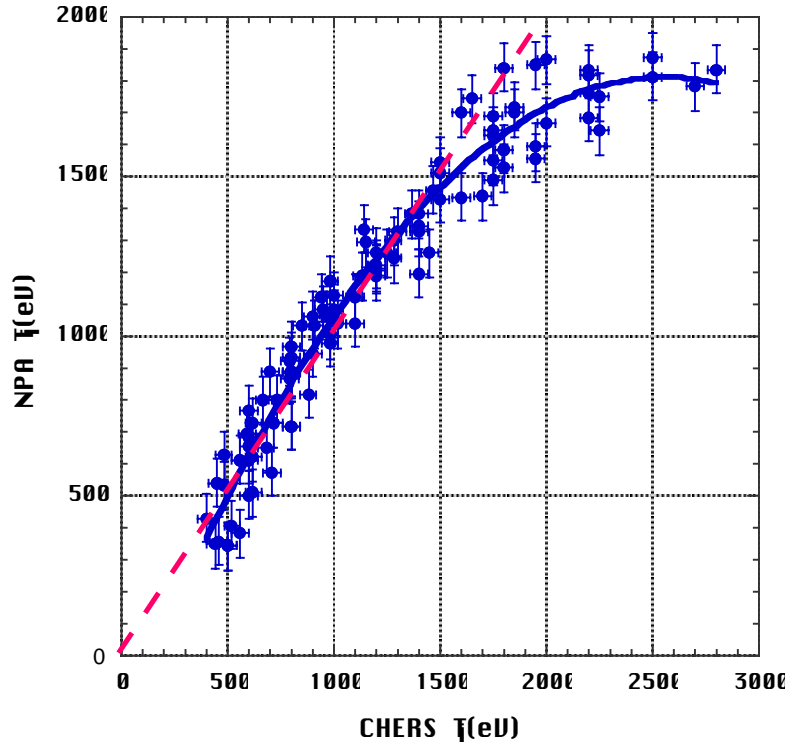

Figure 3. Comparison of ion temperature measurements from the NPA and CHERS diagnostics. The solid curve is a simple fit to the data while the dashed line corresponds to equality between the two measurements.

in the energy range $E/T_i(0)$ ~ 2 – 5. This leads to T_i < $T_i(0)$ at significantly lower $\bar{n}_e$, experimentally determined to be $\bar{n}_e$ ~ 3 x 10^{19} cm^{-3} corresponding to n_eL ~ 3.5 x 10^{19} m^{-2} in the center panel of Figure 2. This interpretation of the NPA ion temperature behavior was verified by application of the neutral particle analysis code DOUBLE to the situation as described in the next section.

3.0 Analysis of NPA Thermal Ion Measurements using the DOUBLE Code

The DOUBLE code[4] was developed at the Ioffe Institute to calculate neutral particle flux escaping from a plasma and detected by a neutral particle analyzer. This is accomplished in two steps: first the neutral particle density distribution over the plasma volume is calculated and then integration along the NPA line of sight is performed.

4

The Bolzmann kinetic equation describing the neutral particle distribution $f(\vec{x}, \vec{v})$ over position, $\vec{x}$, and velocity, $\vec{v}$, space is assumed to be time-independent:

$$\vec{v}\frac{\partial f(\vec{r}, \vec{v})}{\partial \vec{r}} + n_e f(\vec{r}, \vec{v}) \langle \sigma v \rangle_e + f(\vec{r}, \vec{v}) \int \varphi_i(\vec{r}, \vec{v}') \sigma_{CX}\left(|\vec{v} - \vec{v}'|\right)|\vec{v} - \vec{v}'|dv' =$$
$$\varphi_i(\vec{r}, \vec{v}) \int f(\vec{r}, \vec{v}') \sigma_{CX}\left(|\vec{v} - \vec{v}'|\right)|\vec{v} - \vec{v}'|dv' + n_e \varphi_i(\vec{r}, \vec{v}) \langle \sigma v \rangle_r + S(\vec{r}, \vec{v})$$

(1)

where $\varphi_i(\vec{r}, \vec{v})$ is the ion velocity distribution function, $\langle \sigma v \rangle_e$ and $\langle \sigma v \rangle_r$ are the electron ionization and recombination rate coefficients correspondingly, n_e is the electron density, σ_{CX} is the charge exchange cross-section and $S(\vec{r}, \vec{v})$ is the neutral source distribution function. The source term may include local neutral particle sources such as pellet or neutral beam injection. Other neutral sources generated by wall recycling are allowed for in boundary conditions. It must be stressed that all of the distribution functions when integrated over both parameters give corresponding particle densities.

The kinetic equation generally can be solved in two ways. Firstly it can be reduced to an integral equation for the neutral density using a simplified plasma model, e.g., one-dimensional geometry, delta-function as the ion velocity distribution, simplified boundary conditions (uniform wall flux resulting from recycling process). The integral equation then can be solved numerically. This method will be referred to as an analytic one. An alternative approach is to use Monte Carlo methods to integrate the kinetic equation. This is a very powerful tool for including the complicating effects of asymmetries, Maxwellian (and non-Maxwellian) plasmas, and detailed atomic and wall physical processes.

Charge exchange atomic flux escaping the plasma is given by

$$J_a(E) = \int\limits_{LOS} \langle \sigma v \rangle_{CX} n_0(\vec{r}) \varphi_i(\vec{r}, E) \mu(\vec{r}, E) dl$$

(2)

where n_0 is the neutral particle density obtained previously, $\mu(\vec{r}, E)$ is the plasma attenuation factor for a neutral formed in a charge exchange event and E is the neutral energy.

The analytic approach was implemented in the code called DOUBLE. The code simulates three species (two hydrogen and one helium), one-dimensional (cylindrical), stationary plasma. The integral equation for neutral density is solved using the method of successive approximations. Neutral edge density and edge temperature are used as uniform boundary conditions. Although the passive neutral density distribution is simulated in one-dimensional geometry, the rest of the code uses 3D geometry.

In order to simulate NSTX NPA experimental data some modifications to DOUBLE code have been made. The core part of the code that deals with neutral particle transport and calculates the passive neutral density distribution was not affected. The code was modified to simulate horizontal

propagation of the three neutral beam sources in the midplane on NSTX, active charge-exchange events of plasma ions on the three energy components of the beam primary neutrals (and halo neutrals) and the outgoing neutral flux attenuation. The beam density was treated as a two-dimensional Gaussian distribution given by

$$n(x, y) = \frac{N \cdot \exp\left(-\dfrac{x^2}{ew^2} - \dfrac{y^2}{eh^2}\right)}{\pi \cdot ew \cdot eh \cdot \mathrm{erf}\left(\dfrac{fw}{2ew}\right) \cdot \mathrm{erf}\left(\dfrac{fh}{2eh}\right)}, \tag{3}$$

where fw and fh are beam full width and full height, ew and eh are e-folding half widths in radial and vertical direction correspondingly, N is beam linear density. The halo neutral density (1st generation) was deduced from the following balance equation:

$$n_{beam} n_i \cdot \sigma_{cx} v_{beam} = \frac{n_{halo}}{\tau} \tag{4}$$

where τ stands for halo neutral "lifetime" (typical time for a halo neutral to be ionized). The left-hand part represents halo neutral formation rate (gain) and the right-hand part gives the decay rate (loss). Neutral flux produced by charge-exchange events on halo neutrals can be found in the same manner as in the case of the primary beam neutrals. The angle between beam direction and that of the NPA sightline is assumed to be 90 degrees and the NPA sightline is also constrained to lie in the midplane.

To estimate active NPA flux, the code at first calculates the beam attenuation factor along its chord and the corresponding neutral density value is used in the integration procedure along the NPA sightline while taking into account charge-exchange reaction rate. Only the beam-sightline intersection region in the plasma contributes to the active flux.

The attenuation factor (i.e. the probability for a neutral penetrating plasma from its surface to reach the $\vec{r}$ point or the probability for a neutral starting from the $\vec{r}$ point to leave plasma column) can be represented by:

$$\mu(\vec{r}) = \exp\left(-\frac{1}{v}\int_{(L)}^{\vec{r}} n < \sigma v >_{att} dl\right) \tag{5}$$

(where v is the neutral velocity). The emissivity is given by

$$\varepsilon_{act}(\vec{r}, E) = \frac{1}{4\pi} n_{beam}^0 \cdot \mu_{beam}(\vec{r}) \cdot n_i \sigma_{cx} v_{beam} \cdot \varphi_i(E) \tag{6}$$

where n_{beam}^0 is the initial beam density, $\varphi_i(E)$ is plasma ion energy distribution (e.g. Maxwellian). So the active flux is given by

$$J_{act} = \int_{(L_{NPA})} \varepsilon_{act} \cdot \mu_0 dl \cdot \tag{7}$$

6

The inputs to the code include geometrical parameters for the NSTX device and the layout of the neutral beams and the NPA diagnostic. The plasma is characterized by electron density, electron temperature and ion temperature profiles, effective charge value, major and minor radius values etc. The profile data, an example of which is given in the bottom panel in Figure 2, is usually parameterized in a parabolic form:

$$T(r) = T(0) \cdot \left(1 - \left(\frac{r}{a} \right)^{Y1} \right)^{Y2}. \quad (8)$$

The main outputs are neutral particle radial profiles, the so-called emissivity functions and the neutral spectra. The emissivity function represents the probability that a neutral particle of particular energy born at particular location escapes the plasma volume.

The DOUBLE code was used to simulate the NPA measurements for NSTX discharge SN106031 at times t ~ 200 msec and t ~ 270 msec as indicated by the dashed vertical lines in Figure 2. The calculated emissivity function including active beam primary and halo neutrals and passive neutrals is shown in
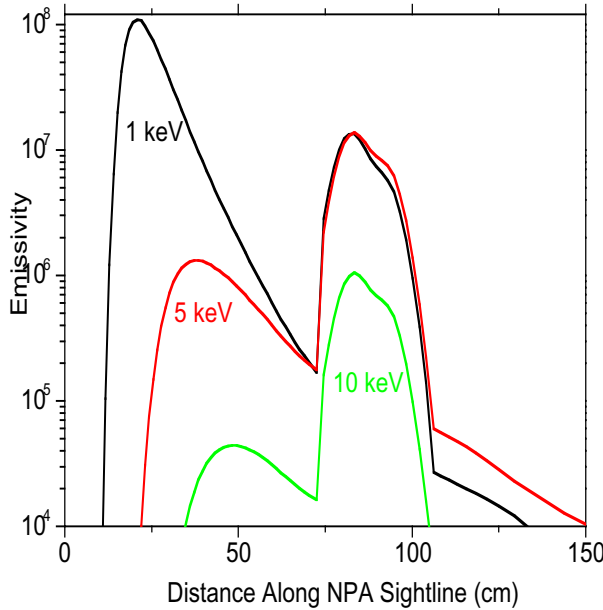

Figure 4. Example of the emissivity calculated by the DOUBLE code, including passive and active neutral particle sources, versus distance along the NPA sightline.

Figure 4 for the charge exchange emission at energies of 1, 5 and 10 keV. The contribution from the neutral beams (Sources B and C) is evidenced by the peaks in the region of 75 – 100 cm along the NPA sightline. The minority hydrogen spectra for the NPA measurements (solid squares) and the DOUBLE code simulations (solid and dashed lines) are shown in Figure 5 for discharge time t ~ 200 msec and in Figure 6 for t ~ 270 msec. In Figure 5, the individual contributions from neutral beam sources B and C and the passive neutrals to the total spectrum are shown. Good agreement is obtained with T_{code} ~ 1500 eV compared with $T_{CHERS,NPA}$ ~ 1500 eV from Figure 2 which benchmarks proper functioning of the code. In Figure 6, the core input temperature to the code was varied between 1300 eV and 2300 eV. The best code fit to the NPA data is obtained with T_{code} ~ 1700-2000 eV compared with the measured CHERS value of T_{CHERS} = 1900 eV. As seen in Figure 2, the ion temperature obtained from the slope of the measured NPA spectrum was considerably lower at T_{NPA} = 1400 eV. Thus the DOUBLE code modeling of the NPA measurements at high n_eL restores agreement with the CHERS Ti(0).
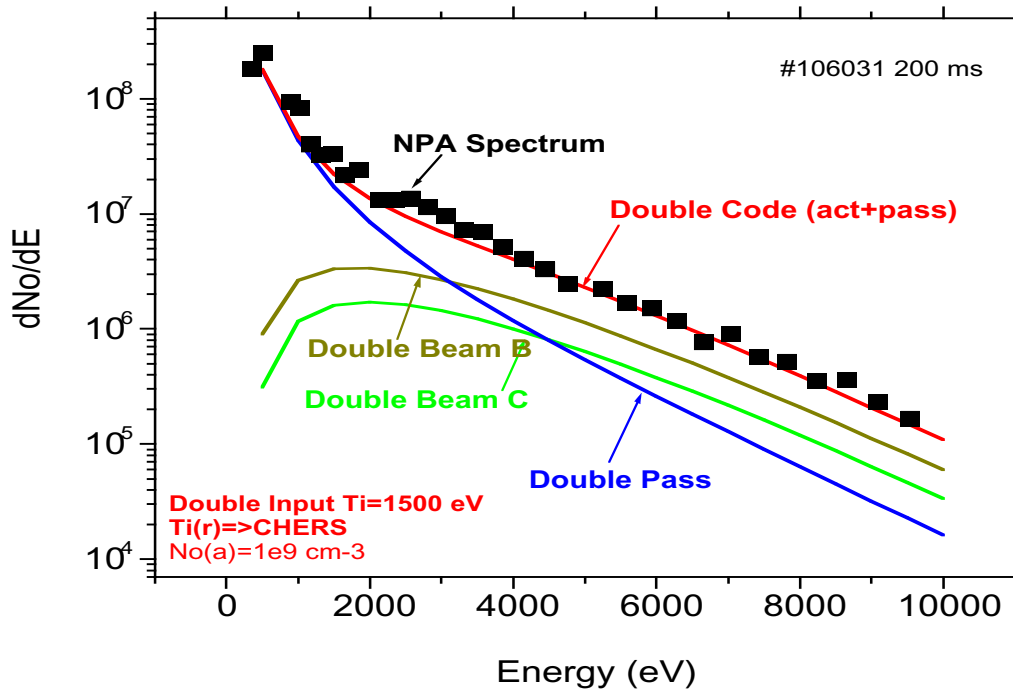
Figure 5 DOUBLE code modeling of the NPA thermal hydrogen ion spectrum (solid squares), including passive and active neutral particle sources, at t ~ 200 msec.
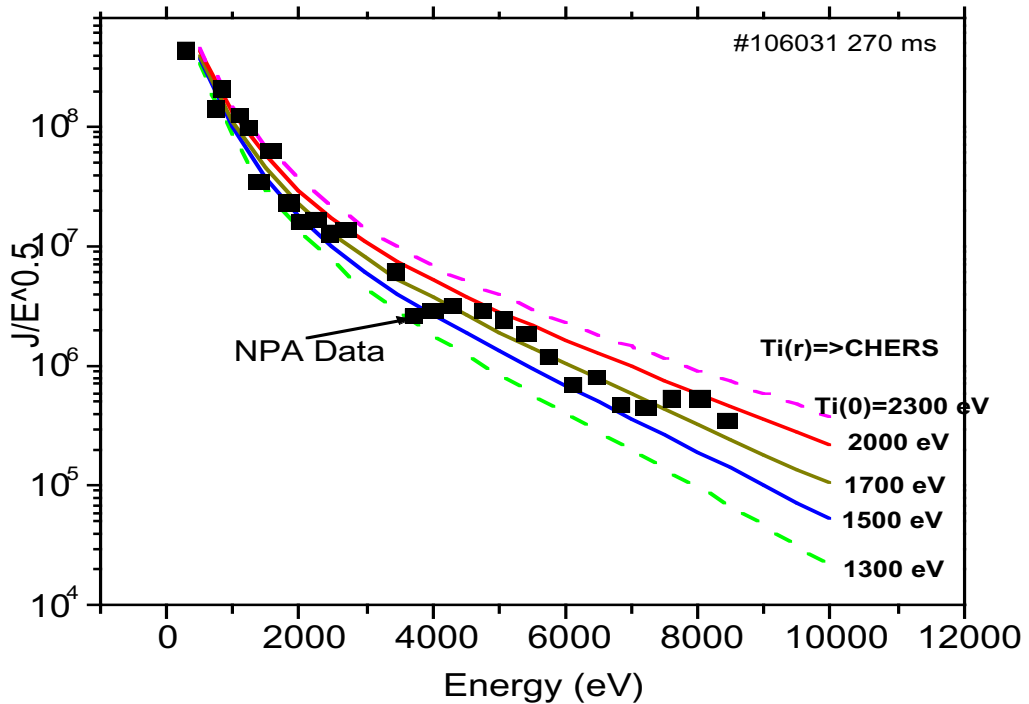

Figure 6. DOUBLE code modeling of the NPA thermal hydrogen ion spectrum (solid squares)at t ~ 270 msec with variation of Ti(0) demonstrating the fit sensitivity.

4.0   Effect of MHD Activity on Thermal Ion Distributions

The appearance of magnetohydrodynamic (MHD) mode activity can have a pronounced effect on both the 'thermal' (E ~ 0.5–10 keV) and 'energetic' (E ~ 10 - 100 keV) ion populations in NSTX. An example is presented in Figure 7 marked by the shaded vertical bar where panel (a) shows injection of a peak NB power of 1.2 MW during the 1 MA flat top of a deuterium discharge. Panel (b) shows the onset of large scale MHD activity at t ~ 0.26 sec as indicated by the Mirnov coil measurements. Note that $q(0) \leq$ 1 during this MHD activity. This activity is identified as an n = 2 mode with frequency ~ 20 kHz. As reported elsewhere [5], growth of the n = 2 mode leads to rollover and relatively slow decay of the energetic ion population and consequently the neutron yield as shown in panel (c). Panel (c) shows thermal ions are also lost during MHD activity which results in a collapse in the ion temperature as seen in panel (d).

The effects of Internal Reconnection Events (IREs) and sawteeth on the thermal and energetic ion distributions in NSTX differ from that observed for MHD mode activity. IREs are signatured by sharp upticks on the plasma current waveform (marked by dashed vertical lines). IREs are also evidenced as a sharp signal burst on the Mirnov waveform whereas other MHD activity exhibits more continuous signal fluctuations. In most cases, strong IREs are preceded by sawteeth or other MHD activity. At an IRE event, prompt loss of the energetic ions occurs on a fast time scale of ≤ 2 msec [5] while the thermal ions remain confined but are redistributed outboard
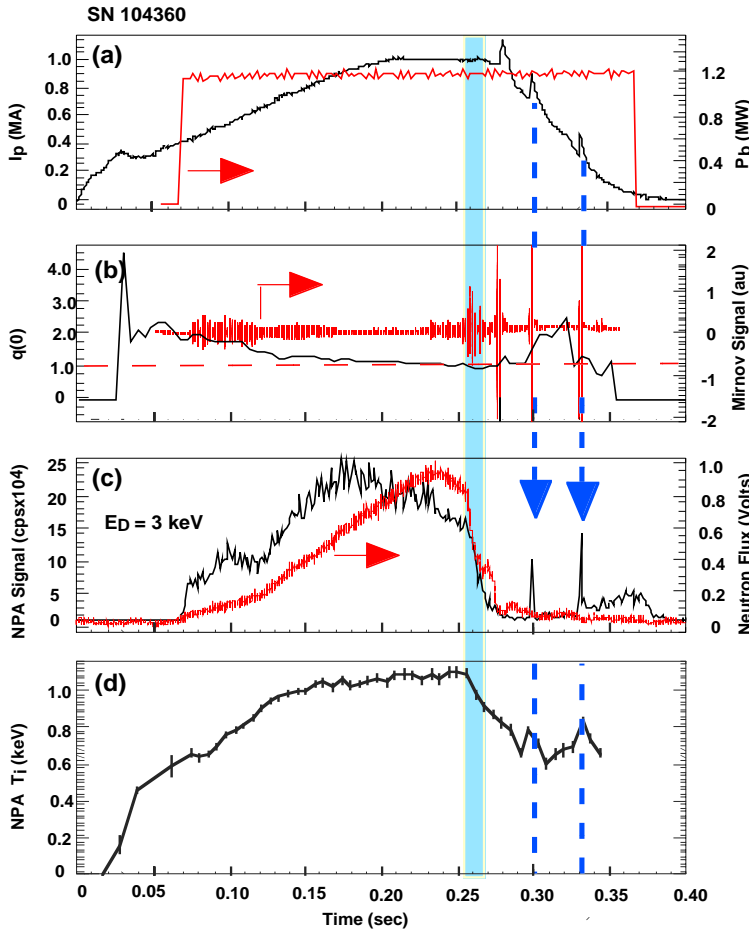
Figure 7. Illustration of the effects of MHD activity and internal reconnection events on the thermal ion distribution measured by the NPA diagnostic in NSTX

9

from the plasma core to a region of higher neutral density which leads to a burst in the neutral particle flux measured by the NPA as seen during the current rampdown at t ~ 0.30 sec and t ~ 0.33 sec in panel (c). Also a small increase in the apparent ion temperature can be seen in panel (d) at the time of the IREs. These observations are indicative of a redistribution of core ions to the plasma periphery where the neutral density is higher, thus producing the spike in the NPA flux and measured T_i. For reasons yet unknown, IREs occasionally have no effect on the NPA signal as can be seen for the IRE at the end on the current flattop in Figure 7.

The best way to determine if the rollover in the NPA ion temperature is due to MHD activity as marked by the shaded vertical bar in Figure 7 or due to the increasing plasma density as in Figure 2 is to inspect the neutron waveform. MHD activity causes the neutron yield to rollover, but increasing plasma density does not.

Acknowledgements

References

1. S. S. Medley, et al., Rev. Sci. Instrum. **69**, 2651 (1998).

2. R. E. Bell, et al., PPPL Report "Kinetic Profiles in NSTX Plasmas," PPPL-3591 (1998).

3. Yu. N. Dnestrovskij, et al., Nucl. Fus. **19**, 293 (1979).

4. A. I. Kisylakov, M. P. Petrov and E. V. Suvorkin, Plasma Phys. Control. Fusion
    43, 1775 (2001).

5.   S. S. Medley, et al., PPPL Report "Neutral Particle Analyzer Measurements of Ion Behavior in
     NSTX," PPPL-3668 (2002)

External Distribution

Plasma Research Laboratory, Australian National University, Australia

Professor I.R. Jones, Flinders University, Australia

Professor João Canalle, Instituto de Fisica DEQ/IF - UERJ, Brazil

Mr. Gerson O. Ludwig, Instituto Nacional de Pesquisas, Brazil

Dr. P.H. Sakanaka, Instituto Fisica, Brazil

The Librarian, Culham Laboratory, England

Library, R61, Rutherford Appleton Laboratory, England

Mrs. S.A. Hutchinson, JET Library, England

Professor M.N. Bussac, Ecole Polytechnique, France

Librarian, Max-Planck-Institut für Plasmaphysik, Germany

Jolan Moldvai, Reports Library, MTA KFKI-ATKI, Hungary

Dr. P. Kaw, Institute for Plasma Research, India

Ms. P.J. Pathak, Librarian, Insitute for Plasma Research, India

Ms. Clelia De Palo, Associazione EURATOM-ENEA, Italy

Dr. G. Grosso, Instituto di Fisica del Plasma, Italy

Librarian, Naka Fusion Research Establishment, JAERI, Japan

Library, Plasma Physics Laboratory, Kyoto University, Japan

Research Information Center, National Institute for Fusion Science, Japan

Dr. O. Mitarai, Kyushu Tokai University, Japan

Library, Academia Sinica, Institute of Plasma Physics, People's Republic of China

Shih-Tung Tsai, Institute of Physics, Chinese Academy of Sciences, People's Republic of China

Dr. S. Mirnov, TRINITI, Troitsk, Russian Federation, Russia

Dr. V.S. Strelkov, Kurchatov Institute, Russian Federation, Russia

Professor Peter Lukac, Katedra Fyziky Plazmy MFF UK, Mlynska dolina F-2, Komenskeho Univerzita, SK-842 15 Bratislava, Slovakia

Dr. G.S. Lee, Korea Basic Science Institute, South Korea

Mr. Dennis Bruggink, Fusion Library, University of Wisconsin, USA

Institute for Plasma Research, University of Maryland, USA

Librarian, Fusion Energy Division, Oak Ridge National Laboratory, USA

Librarian, Institute of Fusion Studies, University of Texas, USA

Librarian, Magnetic Fusion Program, Lawrence Livermore National Laboratory, USA

Library, General Atomics, USA

Plasma Physics Group, Fusion Energy Research Program, University of California at San Diego, USA

Plasma Physics Library, Columbia University, USA

Alkesh Punjabi, Center for Fusion Research and Training, Hampton University, USA

Dr. W.M. Stacey, Fusion Research Center, Georgia Institute of Technology, USA

Dr. John Willis, U.S. Department of Energy, Office of Fusion Energy Sciences, USA

Mr. Paul H. Wright, Indianapolis, Indiana, USA